Journal for ImmunoTherapy of Cancer

Tripartite antigen-agnostic combination immunotherapy cures established poorly immunogenic tumors

Sven Borchmann ,[1,2] Carolin Selenz,[1,2] Mia Lohmann,[1] Hanna Ludwig,[1,2] Asmae Gassa,[3] Johannes Brägelmann,[4] Philipp Lohneis,[5] Lydia Meder,[1,2] Julia Mattlener,[1] Sara Breid,[1,2] Marieke Nill,[1,2] Jana Fassunke,[5] Amy J. Wisdom,[6] Anik Compes,[1,2] Birgit Gathof,[7] Hakan Alakus,[8] David Kirsch,[6] Khosro Hekmat,[3] Reinhard Büttner,[5] H. Christian Reinhardt,[9] Michael Hallek,[1] Roland T. Ullrich[1,2]

To cite: Borchmann S, Selenz C, Lohmann M, *et al*. Tripartite antigen-agnostic combination immunotherapy cures established poorly immunogenic tumors. *Journal for ImmunoTherapy of Cancer* 2022;**10**:e004781. doi:10.1136/jitc-2022-004781

► Additional supplemental material is published online only. To view, please visit the journal online (http://dx.doi.org/10.1136/jitc-2022-004781).

Accepted 18 September 2022

For numbered affiliations see end of article.

Correspondence to
Dr Sven Borchmann, Department I of Internal Medicine and Center for Integrated Oncology, University Hospital of Cologne, Kerpener Str. 62, 50931 Cologne, Germany; sven.borchmann@uk-koeln.de

Prof Roland T. Ullrich, Department I of Internal Medicine and Center for Integrated Oncology, University Hospital of Cologne, Kerpener Str. 62, 50931 Cologne, Germany; roland.ullrich@uk-koeln.de

ABSTRACT

Background Single-agent immunotherapy has shown remarkable efficacy in selected cancer entities and individual patients. However, most patients fail to respond. This is likely due to diverse immunosuppressive mechanisms acting in a concerted way to suppress the host anti-tumor immune response. Combination immunotherapy approaches that are effective in such poorly immunogenic tumors mostly rely on precise knowledge of antigenic determinants on tumor cells. Creating an antigen-agnostic combination immunotherapy that is effective in poorly immunogenic tumors for which an antigenic determinant is not known is a major challenge.

Methods We use multiple cell line and poorly immunogenic syngeneic, autochthonous, and autologous mouse models to evaluate the efficacy of a novel combination immunotherapy named tripartite immunotherapy (TRI-IT). To elucidate TRI-ITs mechanism of action we use immune cell depletions and comprehensive tumor and immune infiltrate characterization by flow cytometry, RNA sequencing and diverse functional assays.

Results We show that combined adoptive cellular therapy (ACT) with lymphokine-activated killer cells, cytokine-induced killer cells, Vγ9Vδ2-T-cells (γδ-T-cells) and T-cells enriched for tumor recognition (CTLs) display synergistic antitumor effects, which are further enhanced by cotreatment with anti-PD1 antibodies. Most strikingly, the full TRI-IT protocol, a combination of this ACT with anti-PD1 antibodies, local immunotherapy of agonists against toll-like receptor 3, 7 and 9 and pre-ACT lymphodepletion, eradicates and induces durable anti-tumor immunity in a variety of poorly immunogenic syngeneic, autochthonous, as well as autologous humanized patient-derived models. Mechanistically, we show that TRI-IT coactivates adaptive cellular and humoral, as well as innate antitumor immune responses to mediate its antitumor effect without inducing off-target toxicity.

Conclusions Overall, TRI-IT is a novel, highly effective, antigen-agnostic, non-toxic combination immunotherapy. In this study, comprehensive insights into its preclinical efficacy, even in poorly immunogenic tumors, and mode of action are given, so that translation into clinical trials is the next step.

WHAT IS ALREADY KNOWN ON THIS TOPIC

⇒ It has been recognized that combination immunotherapy is necessary for the vast majority of tumors as single agent immunotherapy is often insufficient in overcoming resistance mechanisms or low immunogenicity.

WHAT THIS STUDY ADDS

⇒ In this study, we propose a combination immunotherapy that shows high efficacy as well as safety in a wide range of preclinical models of tumors usually responding very poorly to immunotherapy. Importantly, our combination immunotherapy protocol, which we named tripartite immunotherapy (TRI-IT), is universally applicable and does not require prior knowledge of the antigenic determinants of a given tumor.

HOW THIS STUDY MIGHT AFFECT RESEARCH, PRACTICE OR POLICY

⇒ The comprehensive preclinical evaluation of TRI-IT presented within this manuscript provides the basis for immediate clinical evaluation of the TRI-IT protocol.

BACKGROUND

Cancer is a leading cause of morbidity and mortality.[1] While surgery, chemotherapy and radiotherapy have been the core elements of cancer treatment throughout much of its history, immunotherapy has only recently been added to this repertoire.[2 3]

Single-agent immunotherapy, such as immune checkpoint inhibition, has shown remarkable efficacy in some cancers and led to durable remissions in selected patients.[4] However, diverse immunosuppressive mechanisms act in a concerted way to suppress the host anti-tumor immune response. Thus, single-agent immunotherapy is unlikely to be sufficient to overcome these mechanisms,[5] and indeed most human cancers

do not respond to single-agent immunotherapy.[6] In general, tumors responsive to immunotherapy, such as immune checkpoint blockade, have a permissive tumor immune microenvironment (TIME) that is characterized by already existing immune infiltration, active antigen-presentation, and immunogenic cell death.[5] In contrast, poorly inflamed tumors, so called immune-deserts or cold tumors, do mostly not respond to immunotherapy.[7] While some combination immunotherapies have been shown to be effective in preclinical models of such cold tumors, they rely on knowledge of antigenic determinants such as tumor-associated antigens or neoantigens.[8] However, many tumors express few of those and even if present, these are mostly not known for a given patient. Thus, creating an antigen-agnostic combination immunotherapy that is effective in poorly immunogenic tumors for which an antigenic determinant is not known is a major challenge.

Addressing this challenge, we developed an universal combination immunotherapy approach named tripartite immunotherapy (TRI-IT), which combines checkpoint blockade targeting the PD1- axis,[4 9 10] an optimized combined adoptive cellular therapy (ACT) protocol consisting of the transfer of innate and adaptive effector cells with pre-ACT lymphodepletion and local immunotherapy by intratumoral injection of agonists against Toll-like receptor (TLR) 3,7 and 9.[11]

TLRs are highly conserved immune cell receptors that serve as pathogen-associated molecular pattern receptors.[11] TLR3 can be stimulated with Poly I:C, a synthetic double-stranded polyribonucleotide, mimicking double-stranded RNA, a natural agonist for TLR3. TLR3 activation leads to increased CD4+and CD8+ T cell proliferation and survival, increases in γδ-T cell cytotoxicity and stimulation of Interferon γ (IFNγ) and tumor necrosis factor alpha (TNFα) release, leading to local inflammation within the tumor.[11 12] Furthermore, intratumoral TLR3 agonist application can result in autovaccination by eliciting novel antitumor immune responses in the host.[13] TLR7 activation, for example with Gardiquimod, as used in TRI-IT, increases IFNγ and IL-2 production and infiltration of tumors by immune effector cells.[11 12 14] TLR9 can be activated by many CpG oligonucleotides out of which we use ODN2395, a class C CpG oligonucleotide.[15] Activation increases CD4+T cells activity, survival and resistance to inhibitory functions of T regulatory cells (Tregs). TLR9 activation also improves CD4+and CD8+ T cell proliferation by increasing expression of the interleukin 2 receptor (IL-2R) and augmenting IL-2 production.[11 16 17] Our choice of TLR agonists was driven heuristically by prior evidence that their activity might be synergistic with additional synergy on combination with ACT, despite their functional similarity as nucleic acid sensing endosomal TLRs.[11 12 18–21] Low intratumoral dosing is used to avoid systemic effects and toxicity.[22]

Our combined ACT protocol includes lymphokine-activated killer cells (LAKs), cytokine-induced killer cells (CIKs), Vγ9Vδ2-T-cells (γδ-T-cells) and T-cells enriched for tumor recognition (CTLs). LAKs are IL-2 stimulated peripheral blood lymphocytes that obtain unspecific anti-tumor activity in culture. Early human trials with LAKs were promising, however, the concept of using LAKs as a monotherapy was abandoned, because activity was limited and not superior to giving IL-2 directly to patients.[23 24] CIKs are peripheral blood lymphocytes pre-treated with IFNy and expanded with an anti-CD3 antibody and IL-2. Compared with LAKs these have order of magnitude higher expansion, retainment of T cell receptor (TCR) specificity and longer viability in vivo, however they contain fewer expanded NK cells.[25 26] Clinical trials with CIK cells as monotherapy delivered mixed results with more efficacy of CIKs when used in an adjuvant setting with low remaining tumor mass.[27 28] Vγ9Vδ2-T cells are T cells whose TCR consists of a paring of a Vγ9 and Vδ2 chain.[29] These T cells can be considered part of the innate immune system building a bridge towards adaptive immunity.[29] They respond in a non-major histocompatibility complex (MHC)-restricted manner to unconventional antigens, such as phospholipid antigens.[29] First clinical evaluations of γδ-T cells in cancer have resulted in promising first hints at efficacy and a whole range of clinical trials are currently under way.[30 31] For a tumor-specific ACT element, we included CTLs derived with a novel co-culture method that enriches for tumor-reactive, tumor-specific cytotoxic T lymphocytes.[32 33] Lymphodepletion was added to TRI-IT based on the necessity to deplete competing host lymphocytes in a wide range of cellular therapy approaches such as tumor infiltrating lymphocytes (TILs) or chimeric antigen receptor (CAR)-T cells.[34 35] Due to their diverse mechanism of action, we hypothesized that a combined ACT protocol consisting of these components will be synergistic compared with single ACT therapy and overcome the known limitations of single component ACT.

Here, we present the results of a comprehensive preclinical evaluation of TRI-IT's efficacy and mechanism of action.

METHODS

Statistics

Statistical analyses and data visualization were performed with R[36] and Graphpad.[37] Statistical tests used are indicated in figure legends or throughout the text.

Cell lines

The murine melanoma cell line B16F10 was kindly provided by Hans Schlößer (University of Cologne, Germany), the Hodgkin lymphoma cell lines L428, L540, L1236 and KMH2 were kindly provided by Hinrich Hansen (University of Cologne, Germany). The human lung cancer cell lines H1975 and H441 were obtained from ATCC (Manassas, VA). JimT1 was obtained from DSMZ (Leipzig, Germany). The Kras/p53-null (KP) and methylcholanthrene (MCA)-induced/p53-null (MCA/p53) sarcoma cell lines were kindly provided by David

Kirsch (Duke University, North Carolina, USA). The murine lung cancer cell line KP 938.3, generated by culturing $Kras^{LSL\text{-}G12D}$ $p53^{fl/fl}$ tumors in vitro, was kindly provided by Christian Reinhardt (University of Essen, Germany). Some cell lines were transduced to stably express firefly luciferase for cell viability monitoring by luminescence.[38]

All cell lines were cultured in a 50%/50% v/v mixture of RPMI-1640 (Gibco, Carlsbad, CA) and DMEM-F12 (Gibco) supplemented with 10% fetal bovine serum (FBS) and 100 U/mL penicillin (Gibco) and 100 µg/mL streptomycin (Gibco). All cell lines were cultured, and all in-vitro assays performed at 37°C and 5% CO2. Cell lines were regularly tested for mycoplasma contamination.

Tripartite immunotherapy

TRI-IT consists of three treatment components. The first component is ACT of a combined cell therapy product consisting of LAKs, CIKs, Vγ9Vδ2-T-cells and in vitro enriched, tumor-specific T-cells (CTLs). Cells were given in equal proportion as part of the combined treatment, meaning a quarter of the given number of cells consisted of each cell type. The cell dose was heuristically determined and 1×10^7 cells in up to 200 µl of PBS were injected i.p. per dose. To support engraftment, cellular therapy was followed by five daily doses of 1×10^5 IE recombinant interleukin (IL)-2 (Aldesleukin, Novartis, Basel, Switzerland) in up to 100 µL PBS s.c. The second component is systemic immune checkpoint inhibition by i.p. injection of 5 mg/kg of either anti-mouse aPD1 antibody (clone RMP1-14, BioXCell, Lebanon, New Hampshire, USA) or clinical-grade Nivolumab (Bristol-Myers-Squibb, New York, New York, USA) in 100 µl PBS per dose. Two doses per week were given. The third component is local immune stimulation by a mix of agonists against TLR3, TLR7 and TLR9. The agonists used were Poly I:C (Millipore, 1.25 mg/kg/BW), Gardiquimod (Cayman Chemical, Ann Arbor, Michigan, USA, 1.25 mg/kg/BW) and ODN-2395 (5'-tcgtcgttttcggcgcgcgccg-3' with phosphorothioate bonds, synthesized by IDT, Coralville, IA, 1.25 mg/kg/BW). These were given twice weekly diluted in PBS intratumorally (or peritumorally if tumors were too small to be directly injected) per dose. Unless indicated otherwise, only the right tumor was injected to model injection of only one lesion in a patient. In one experiment TLR agonists were given inhaled at similar concentrations after isoflurane anesthesia.

If lymphodepletion was given, it consisted of clinical-grade cyclophosphamide (HEXAL, Holzkirchen, Germany, 200 mg/kg/BW) and clinical-grade fludarabine (Sanofi Genzyme, Paris, France, 40 mg/kg/BW) given i.p. in 100 µL PBS 24 hours before treatment began. If an experimental group included only a subset of treatments, the other treatments were substituted with appropriate controls. These were either identically applied PBS injections or appropriate IgG controls for aPD1-antibody treatment (Isotype control rat IgG2a, κ (BioXCell) for murine a-PD1 and clinical-grade human IgG (Octagam, octapharma, Lachen, Switzerland) for Nivolumab.

Animal experiments

Experiments were performed in accordance with FELASA recommendations. The protocol was approved by the local animal ethics committee for the jurisdiction (Landesamt für Natur, Umwelt und Verbraucherschutz Nordrhein-Westfalen - LANUV NRW, approval no. 84-02.04.2015.A172, 84-02.04.2017.A236, 84-02.04.2018.A368, 81-02.04.2020.A026, §4.21.024, and 81-02.04.2020.A219). Mice were housed and all experiments performed in a sterile environment. Mice were fed, given water and monitored daily for health, and cages were changed weekly.

In vivo tumor growth experiments

For the subcutaneous B16F10 melanoma model, 8–12 week-old C57BL/6J mice were inoculated subcutaneously with 5×10^5 B16F10 melanoma cells in each flank in 100 µL in PBS. Treatment was initiated on day 10 after inoculation on which tumors had an average size of 50–100 mm^3.

For the subcutaneous KP lung cancer melanoma model, C57BL/6J mice aged 8–12 weeks were inoculated subcutaneously with 5×10^6 KP938.3 cells in each flank in 100 µL in PBS. Treatment was initiated on day 10 after inoculation on which tumors had an average size of 50–100 mm^3.

For the subcutaneous sarcoma models, 129/SvJ mice aged 8–12 weeks were inoculated subcutaneously with 2×10^5 MCA/p53 or KP sarcoma cells in each flank in 100 µL in PBS. Treatment was initiated on day 10 after inoculation on which tumors had an average size of 50–100 mm^3.

Tumor growth was measured twice weekly by caliper measurement of the longest diameter l and an orthogonal measurement s. Tumor volume was estimated with the following formula:

$$\frac{S^2\times l}{2}$$

The fold change of tumor growth was calculated by dividing the tumor volume of a specific measurement by the initial tumor volume to account for differences in initial tumor volume.[39]

Autochthonous non-small cell lung cancer model

As a well-established autochthonous model for KRAS-mutant lung adenocarcinomas, we used $Kras^{LSL\text{-}G12D}$ $p53^{fl/fl}$ (KP) mice as described previously.[40] Tumor induction was performed in KP mice aged 6–8 weeks using a type 2 alveolar epithelial cell-specific Adenovirus-Cre (Ad5mSPC-Cre from Viral Vector Core, University of Iowa/Anton Bern, NKI). Mice were anesthetized with Ketamine/Xylazine (100 mg/kg body weight and 10 mg/kg body weight, respectively, i.p.) and 2×10^7 pfu Adenovirus-Cre were administered intranasally, as previously described.[40] Four weeks after virus inhalation, lungs were scanned by µCT to confirm tumor formation. Subsequently, tumor

progression was monitored by weekly µCT scans with a LaTheta LCT-100 small animal µCT (Hitachi Aloka Instruments, Tokyo, Japan). CT images of the whole lung were taken at 0.3 mm intervals and analyzed using InVesalius 3.0 software (Amsterdam, Netherlands).

Autologous humanized patient-derived xenograft models

Tumor material was obtained from consenting non-small cell lung cancer (NSCLC) patients. To establish first-generation patient-derived xenograft (PDX), the tumor specimen was transported sterile directly from surgery to the animal facility in RPMI-1640 (Gibco) supplemented with 10% FCS and penicillin-streptomycin, where it was dissected into 3×3×3 mm large pieces. Subcutaneous pockets were prepared in both flanks of 8–12 weeks NSG (NOD.Cg-Prkdcscid Il2rgtm1Wjl/SzJ) mice in general anesthesia and one piece was tumor tissue was inserted into the prepared pocket. At the end of the procedure, the skin is closed with adhesive and mice received adequate postsurgical care with daily wound controls and analgesia. Once tumors were established, growth was monitored. When tumors reached a size of about 1 cm in their largest diameter, they were transplanted as described above into the next generation of mice. A PDX model was considered stable, when it had been transplanted at least three times and the fourth generation was the earliest generation, in which mice were used for experiments.

In parallel, we generated cell lines from tumors by mashing one 3×3×3 mm large tumor fragment with three parallel sterile scalpel blades and transferring the resulting mashed tissue into cell culture plates filled with a 50%/50% v/v mixture of RPMI-1640 (Gibco) and DMEM-F12 (Gibco) supplemented with 10% FBS and penicillin-streptomycin. We used large cell culture plates filled with at least 50 mL of medium. Cells were left untouched for 3 days. On day 3, half the medium was exchanged carefully for fresh medium. Cultures were monitored for emergence of adherent tumor cell clusters. Once these were identified, all medium was removed, and culture plates were washed with PBS before continuing the culture with new medium. Cells were only split by trypsinization if they were fully confluent. We observed a reduction of proliferating fibroblasts and dominance of tumor cells over time in successful cultures, whereas only fibroblasts proliferated after some time in unsuccessful cultures and ultimately stopped proliferating as expected.

For tumor growth experiments, mice were humanized with 2.5×10^6 autologous PBMCs (peripheral blood monolculear cells) i.p. on the same day as they were transplanted with a PDX fragment as described above. Treatment (as described above in 'TRI-IT') was initiated on days 10–16 depending on the PDX model once tumors reached an average size of 50–100 mm^3.

Long-term tumor control and rechallenge experiments

Mice were inoculated subcutaneously with one B16F10 or KP938.3 tumor as described above. Two full treatment cycles were given starting on day 10 after inoculation. These consisted of lymphodepletion followed 24 hours later by ACT followed by 3 days of s.c. IL-2 to support engraftment. After ACT, systemic immune checkpoint inhibition targeting PD1 and local immunotherapy with the TLR-agonist mix was given twice weekly as described above. Another, identical treatment cycle was given on day 27. All treatment was stopped on day 49. On day 60, mice were rechallenged with B16F10 or KP938.3 cells, respectively. No further treatment was given, and mice were observed for tumor growth until day 120.

Synergy of adoptive cellular components in vivo

For studying the synergy of ACT components, mice were either treated with 1×10^7 cells of quadruple (LAKs, CIKs, γδT-cells and CTLs) ACT or with each component on its own or dual or triple subcombinations so that a total of 1×10^7 cells were applied with equal parts of each single effector cell component given. Lymphodepletion was applied in the B16F10 model.

Evaluation of TRI-IT toxicity

Toxicity of TRI-IT was evaluated in the subcutaneous B16F10 melanoma model. Mice were divided into four groups: TRI-IT+B16F10 inoculation, IgG/PBS control+B16F10 inoculation, TRI-IT+mock tumor inoculation (PBS only) and IgG/PBS control+mock tumor inoculation (PBS only). Mice were weighed twice weekly starting before treatment initiation (day 10). On day 24, mice were euthanized, organs harvested, weighed, and fixed for immunohistochemistry (IHC) in 4% PBS-buffered formalin.

Additional methods

Additional methods are available as online supplemental methods in the accompanying supplement.

RESULTS

Combined ACT displays synergistic antitumor activity

To investigate whether the presence of diverse effector cells in the TIME is associated with improved patient outcome, we used CIBERSORT[41] on TCGA data to construct a straightforward heuristic score with one point given for above median infiltration of T-cells excluding γδ-T-cells, NK-cells and γδ-T-cells. CIBERSORT is a well-validated tool to deconvolute immune cell abundances in tumors.[41] We found that combined tumor infiltration of these cells, as measured by our score, is a better predictor of prolonged overall survival than infiltration by any of the score components (online supplemental figure S1A-E) in an all-cancer cohort (online supplemental figure S1A) as well as in entity-specific subgroups, such as lung cancer (online supplemental figure S1B), melanoma (online supplemental figure S1C), and sarcoma (online supplemental figure S1D).

Thus, we hypothesized that a combination of ACT components representing these innate and adaptive effector cells might display synergistic efficacy against tumor cells. Specifically, we combined three innate-acting,

functionally diverse, largely MHC-unrestricted effector cell types with partly distinct recognition mechanisms, LAKs (ie, IL-2 stimulated PBMCs),[42] CIKs (ie, IFNγ-pretreated, anti-CD3 and IL-2 stimulated PBMCs)[25] and Vγ9Vδ2-T-cells (γδ-T-cells, ie, PBMCs selectively stimulated with zoledronic acid and IL-2)[43] with tumor-specific, MHC-restricted cytotoxic T-lymphocytes (CTLs).[32 33] Of note, tumor specific CTLs were generated by a recently published coculture method[33] which did not require prior knowledge of any tumor-associated or neoantigen as for example CAR-T-cells do. Thus, CTLs were tumor-specific, yet antigen-agnostic.

First, we tested whether combined ACT of these innate and adaptive effector cells is more efficacious than single cell type ACT using in vitro toxicity assays in poorly immunogenic B16F10 melanoma and *Kras*$^{LSL.G12D/wt}$;*Tp53*$^{fl/fl}$-derived (KP) lung cancer models. Of note, these models are poorly immunogenic despite the fact that melanoma and lung cancer are often quite immunogenic in humans.[44] We expanded murine equivalents of these effector cells, which showed the expected phenotype (online supplemental figure S2A), specificity (online supplemental figure S2B-E) and functionality (online supplemental figure S2F) (online supplemental note). These experiments also further supported the rationale of combining the four selected ACT components beyond synergy, as each ACT component has a unique phenotype and mechanism of resistance (online supplemental figure S2A-F). For example, tumors would resist CTL attack when they loose antigen presentation via MHC class I, while such an immune escape by the tumor might at the same time increase their susceptibility to LAKs.

We found increasing synergy in higher-order combinations with the quadruple combination showing maximum synergy as evidenced by a low combination index (figure 1A). As expected, dual and triple subcombinations consisting of both innate-acting (eg, LAKs or CIKs) and tumor-specific effector cells (eg, CTLs) were more synergistic than innate-only combinations (figure 1A). To substantiate these findings in vivo, we tested the synergy of the quadruple combination of LAKs, CIKs, γδ-T-cells and CTLs (Combined ACT) and each subcomponent at the same cell dose—that is, either 1×10^7 cells of a subcomponent or 2.5×10^6 cells of each subcomponent for a total of also 1×10^7 cells—in the B16F10 model (figure 1B). Combined ACT had a stronger inhibitory effect on tumor growth than each ACT subcomponent (figure 1C). To rule out that a dual and triple subcombination of effector cells is sufficient while being less complex than the quadruple combination, we tested all possible dual and triple sub-combinations. These experiments showed that in vivo efficacy of the quadruple combination was higher than all dual and triple subcombinations (online supplemental figure S2G).

To disentangle the effect of combined ACT on the TIME composition, we applied immune cell deconvolution based on 3'mRNAseq of bulk tumor tissue harvested at the end of the experiment. We found a higher infiltration of macrophages, Th1, Th2 and Th17 polarized T-cells, Tfh cells, cytotoxic T-cells and γδ-T-cells into tumors in combined ACT compared with single ACT treated mice (figure 1D).

Next, we analyzed the functional state of the TIME by quantifying intratumoral transcripts of common chemokines and cytokines. We detected higher levels of Eotaxin, M-CSF (macrophage colony-stimulating factor), LIF, MIP-1a, MIP-1b, IP-10 and MIG in combined ACT compared with single ACT treated mice, indicating a broad increase in important antitumor chemo-attractants (figure 1E).

The circulatory cytokine signature was rather similar in all single ACT treated mice, with the exception that IL1b, IL-10 and LIX was detected at higher levels in LAK-treated mice and MIP-2 at higher levels in CTL treated mice. In contrast, TNFα, IFNγ, IL7, IL15, IL17, IP10 and M-CSF (macrophage colony-stimulating factor) were significantly increased in the circulation of combined ACT (figure 1F,G). Together, these data indicate that combined ACT might lead to a more Th1-polarized immune response with high levels of homeostatic cytokines (eg, IL7, IL15) associated with increased NK and T-cell activity, proliferation and survival.[45 46] In contrast, efficacy of single ACT might be limited by high levels of potentially immunosuppressive cytokines (eg, IL10)[47] or LIX, which has recently been described as tumor growth and metastasis promoting.[48 49]

Next, we tested if an aPD1 antibody augments the cytotoxicity of ACT subcomponents. As expected, we found that addition of aPD1 significantly increased cytotoxicity of LAKs, CIKs, γδ-T-cells and CTLs (online supplemental figure S3A) targeting B16F10 melanoma and KP lung cancer in vitro. These results were largely confirmed in human lung- and breast cancer and lymphoma models (online supplemental figure S3B).

To corroborate our findings, we validated the synergy of combined ACT in an alternative, allogeneic human context (see below for validation of allo-specificity of human ACTs). We found in vitro synergy of the combined ACT regimen in JimT1 human breast cancer, H441 and H1975 human lung cancer and L428, L540, L1236 and KMH2 human lymphoma. Again, synergy was mainly observed in combinations of innate-acting and tumor-(allo)-specific effectors (figure 1H). Finally, we tested combined human ACT in a humanized, H1975 lung cancer xenograft model in NSG mice, also observing synergy of combined ACT (figure 1I).

Altogether, these data show that combined ACT of equal numbers of LAKs, CIKs, γδ-T-cells and tumor-specific CTLs is superior to subcomponent single cell type ACT in vitro and in vivo in multiple models and associated with beneficial changes in the TIME. While recognizing the complexity of the quadruple combined ACT, we choose to use it in the further development of TRI-IT because we aimed for a universal combination immunotherapy approach and dual or triple subcombinations were not maximally effective in at least one tested in vitro model (figure 1A,H).

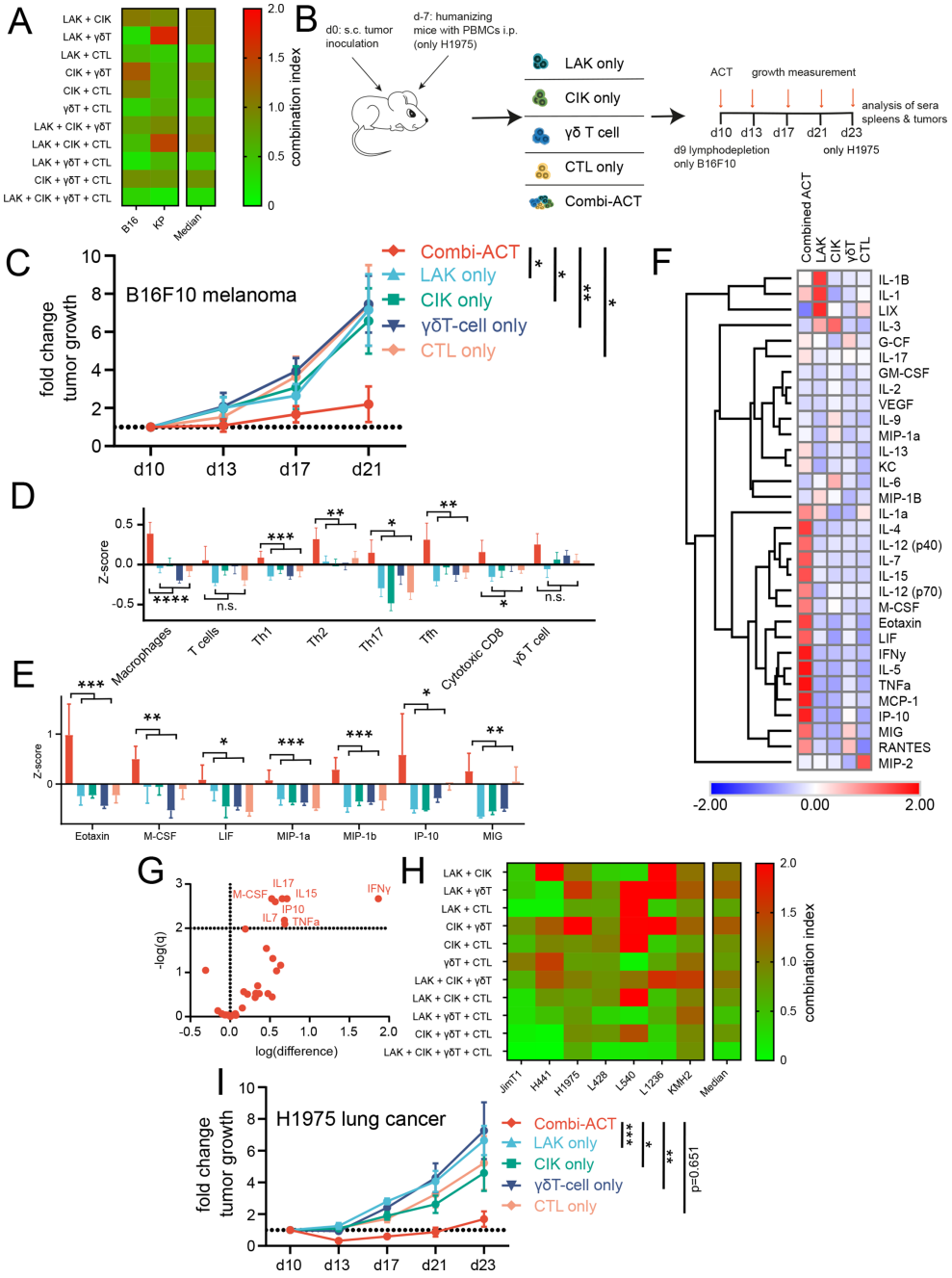

Figure 1 Combined treatment with lymphokine-activated killer cells (LAKs), cytokine-induced killer cells (CIKs), Vγ9Vδ2-T-cells (γδ-T-cells) and adaptive, tumor-specific T-cells (CTLs) is superior to single cell type adoptive cellular therapy. (A) Heatmap of Chou-Talalay combination index (lower equals more synergy) of various adoptive cellular therapy (ACT) subcomponents in two murine cell lines and their median, (B) experimental overview of in vivo experimental workflow for this figure, (C) mean fold change of subcutaneous B16F10 melanoma tumor volumes in C57BL/6J mice over time treated with ACT subcomponents or combined ACT at equivalent doses (n=8 per group), (D) immune cell deconvolution analysis showing mean gene expression z-scores of immune cell specific transcripts (see the Methods section for details), (E) mean gene expression z-scores of intratumoral cytokines and chemokines (n=3–8) per group, B16F10 tumors harvested on day 21 treated in different experimental groups for (D, E), (F) heatmap of mean z-scores of cytokines quantified by multiplex Luminex analysis in the sera of B16F10 bearing C57BL/6J mice sacrificed on day 21 treated in different experimental groups, (G) volcano plot showing cytokines detected at significantly higher levels in combined ACT compared with pooled ACT subcomponent treated B16F10 melanoma bearing C57BL/6J mice, (H) heatmap of Chou-Talalay combination index of various ACT subcomponents in seven human cell lines and their median, (I) mean fold change of subcutaneous H1975 lung cancer tumor volumes in humanized NSG mice over time treated with ACT subcomponents or combined ACT at equivalent doses (n=6–8 per group). all error bars show SE, statistical tests used are two-way ANOVA (C, I), and t-test comparing combined ACT with a pooled control of all single ACT (D, E). *p<0.05, **p<0.01, ***p<0.001, ****p<0.0001. ANOVA, analysis of variance.PBMC, peripheral blood mononuclear cell. M-CSF: macrophage colony-stimulating factor.

TRI-IT eradicates established, poorly immunogenic tumors and induces durable antitumor immunity

We next sought to investigate whether additional activation of TLRs enhances the specific and unspecific effector cell response, improves immune cell recruitment to the tumor site and, thus, improves efficacy of ACT and aPD1 treatment. For these experiments, we used the B16F10 melanoma and KP lung cancer model (figure 2A), as both models are known to be refractory to conventional immunotherapeutic approaches.[50 51] Consistent with previous data, treatment of established (~50–100 mm^3) B16F10 melanomas with single-strategy immunotherapy (aPD1, TLR agonist mix, combined ACT) resulted in only marginally better tumor control compared with IgG/PBS controls (figure 2B). Dual combinations provided only slightly better tumor control then single-strategy immunotherapy, as did the triple combination of aPD1, TLR agonist mix and combined ACT without lymphodepletion. In contrast, triple combination of aPD1, combined ACT with TLR agonist mix including lymphodepletion—the full TRI-IT protocol—led to massive tumor shrinkage in both models (figure 2B,C, online supplemental figure S4A,B).

Motivated by this finding, we investigated long-term tumor control after TRI-IT and treated mice with up to 2 cycles of TRI-IT with survival as the primary endpoint (figure 2D). Strikingly, 71% of animals in the B16F10 (figure 2E) and 70% of animals in the KP model (figure 2F) achieved complete tumor rejection after 60 days.

To assess durable antitumor immunity, we rechallenged these mice on day 60 without further treatment. Remarkably, 83% of B16F10 melanoma (figure 2G) and 100% of KP lung cancer bearing animals (figure 2H) were immune to rechallenge showing no tumor growth.

To assess if local TLR agonist mix treatment is only active locally, we compared injected with non-injected tumors in all groups where the TLR agonist mix was part of the treatment. We observed no difference between injected and non-injected tumor growth in both models (online supplemental figure S4C,D), indicating that local immunotherapy with the TLR agonist mix likely induces systemic, abscopal effects, although at least partial distribution of locally injected TLR agonist to the contralateral tumor site cannot be ruled out.

Taken together, TRI-IT is a highly effective, antigen-agnostic, combination immunotherapy regimen that can cure established, poorly immunogenic tumors and induce durable anti-tumor immunity.

TRI-IT orchestrates a broad antitumor immune response in poorly immunogenic tumors

Motivated by the high efficacy of TRI-IT in two distinctively different, poorly immunogenic tumor models, we aimed to unravel the cellular and molecular mechanisms of TRI-IT. To quantify humoral antitumor immunity, we measured circulating antitumor antibodies. TRI-IT led to high-titer antitumor antibody responses that were higher than in all other groups in both models (figure 3A,B). To quantify cellular anti-tumor immunity of B16F10-bearing mice, we measured cytotoxicity and intracellular IFNγ expression in various splenocyte subsets on coincubation with B16F10 targets. Compared with IgG/PBS and aPD1 treated mice, splenocytes of TLR agonist, combined ACT and TRI-IT-treated mice exhibited higher cytotoxicity (figure 3C). Compared with IgG/PBS and aPD1 treated mice, a significantly higher proportion of CD4+ and CD8+T cells, γδ-T-cells and NK-cells from spleens of TRI-IT-treated mice were IFNγ+ after co-incubation (figure 3D). Together, both assays demonstrate that TRI-IT induces tumor-specific cellular immunity.

Next, we studied the composition of the B16F10 melanoma TIME in different groups by flow cytometry. We observed a pattern of increased infiltration of tumors by T-cells (figure 3E), and more specifically CD8+T cells (figure 3F) with a trend toward increased infiltration by CD4+T cells (online supplemental figure S4E), a higher CD8+T cell/Treg-ratio (figure 3G), and increased infiltration by NK- and NK1.1+CD3+cells (figure 3H,I) in higher order subcombinations. Treg infiltration was similar in all groups (online supplemental figure S4F). Only TRI-IT led to a high γδ-T-cell infiltration (figure 3J).

As IFNγ+ cells in the TIME reflect local anti-tumor immunity better than immune cell quantities,[52] we measured the proportion of IFNγ+ cells of tumor-infiltrating CD4+ (figure 3K) and CD8+T cells (figure 3L), γδ-T-cells (figure 3M), NK-cells (figure 3N) and NK1.1+CD3+cells (figure 3O) by flow cytometry. Only TRI-IT increased the intratumoral proportion of IFNγ+ cells across all immune cell subsets (figure 3K–O).

In KP lung cancer, differences in TIME composition between groups were not as pronounced compared with B16F10 melanoma, though showed similar trends (online supplemental figure S4G–M).

The combination of antibodies directed against PD1 and CTLA4, two clinically well-established immune checkpoints, could potentially be a technically much less complex combination regimen than TRI-IT. Therefore, we wanted to evaluate how this combination performs regarding tumor control in our B16F10 melanoma model, where we treat established tumors. Matching previously published findings in a similar model,[53] we did not observe any significant efficacy of the combination of antibodies against PD1 and CTLA4 in our experiments (online supplemental figure S4N).

To further elucidate the shape of the systemic immune response we measured circulatory cyto- and chemokines. Lymphodepletion led to increased systemic levels of IP-10, MCP-1, MIG and LIX. Local treatment with TLR agonist mix led to increased levels of IL-1b and MIP-1a, while aPD1 treatment led to increased levels of IL-2 and IFNγ, as well as IL-1a, MIP-2, IL-12(p40), M-CSF (macrophage colony-stimulating factor) and VEGF (vascular endothelial growth factor). These signatures where largely maintained when treatments were combined. However, we also found increased systemic levels of cytokines such

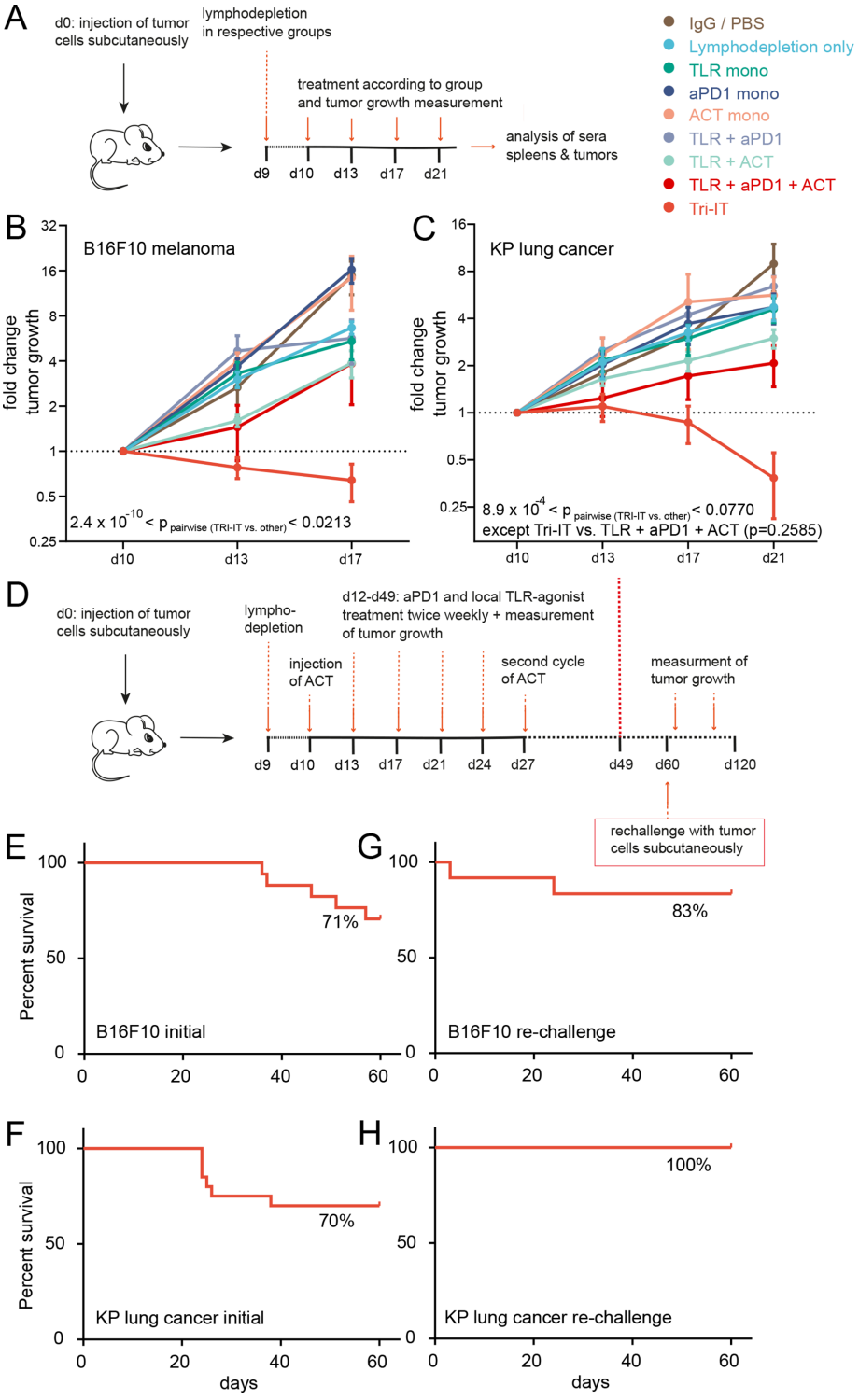

Figure 2 TRI-IT synergistically eradicates established, poorly immunogenic tumors. (A) Experimental overview of in vivo experimental workflow for (B, C), (B) mean fold change of subcutaneous B16F10 melanoma tumor volumes in C57BL/6J mice over time in indicated groups* (n=6–16 per group, pooled from multiple independent experiments), (C) mean fold change of subcutaneous KP lung cancer tumor volumes in C57BL/6J mice over time in indicated groups* (n=5–18 per group, pooled from multiple independent experiments), (D) experimental overview of in vivo experimental workflow for (E–H), (E, F) Kaplan-Meier survival plot of established B16F10 melanoma (E) or KP lung cancer (F) bearing C57BL/6J mice treated with TRI-IT. (G, H) Kaplan-Meier survival plot of previously B16F10 melanoma (G) or KP lung cancer (H) bearing C57BL/6J mice surviving until day 60 after TRI-IT treatment being rechallenged with B16F10 melanoma (G) or KP lung cancer (H). All error bars show SE, statistical tests used are pairwise two-way ANOVA (TRI-IT vs other) (B, C). *The ACT mono groups in (B, C) show reduced tumor growth inhibition compared with figure 1C, because ACT was given without lymphodepletion in these experiments, whereas lymphodepletion was included in figure 1C. ACT, adoptive cellular therapy; ANOVA, analysis of variance; TRI-IT, tripartite immunotherapy. PBS, phosphate-buffered saline. KP, $Kras^{LSL\text{-}G12D}$ $p53^{fl/fl}$ lung cancer cell line.

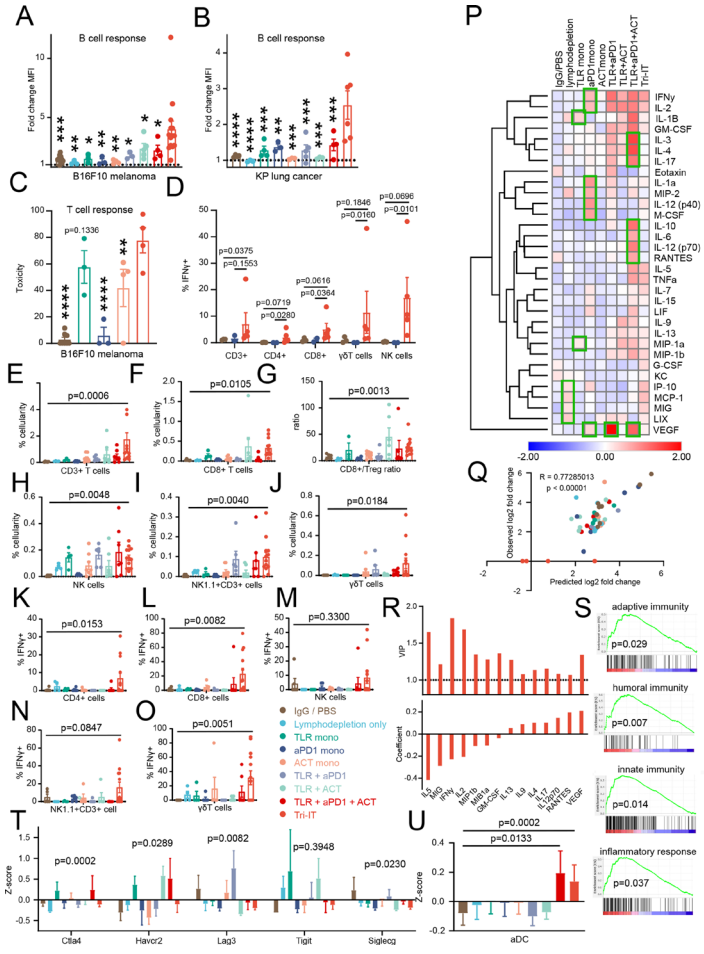

Figure 3 TRI-IT orchestrates a broad antitumor immune response in poorly immunogenic tumors. (A, B) Quantification of antitumor antibody response in sera of subcutaneous B16F10 (A) or KP (B) bearing C57BL/6J mice on day 21 (B16F10) or day 24 (KP) in different treatment groups shown as fold change of geometric mean fluorescence intensity measured by FACS compared with tumor-naïve control mice (n=3–14 per group, pooled from multiple independent experiments, see the Methods section for details,[+]), (C, D) Quantification of cellular antitumor immunity in splenocytes of B16F10 bearing C57BL/6J mice on day 21 in different treatment groups by (C) cytotoxicity toward B16F10 cells (n=3–8 per group, [+]) or (D) intracellular IFNγ response measured by FACS on B16F10 re-stimulation (n=2–5 per group), (E–J) Immune cell infiltration into subcutaneous B16F10 bearing C57BL/6J mice on day 21 in different treatment groups measured by FACS (n=4–13 per group, pooled from multiple independent experiments), (K–O) proportion of IFNγ+ cells among indicated subsets of tumor-infiltrating immune cells in subcutaneous B16F10 bearing C57BL/6J mice on day 21 measured by intracellular FACS (n=4–13 per group, pooled from multiple independent experiments), (P) heatmap of mean z-scores of cytokines quantified by multiplex Luminex analysis in the sera of pooled B16F10 or KP bearing C57BL/6J mice sacrificed on day 21 (B16F10) or day 24 (KP) mice treated in different experimental groups with groups of cytokines altered similarly in a treatment group highlighted in green, (Q) correlation between observed log2 fold change and log2 fold change predicted by the final PLR model using cytokines quantified in sera as inputs to predict end of experiment tumor size (see the Methods section for details), (R) coefficients and VIP scores (measure of importance of input variable in model) for all cytokines with a VIP score >1 in the final PLR model, (S) gene set enrichment analysis of day 24 KP tumors for selected gene sets from TRI-IT-treated mice vs pooled mice from all other treatment groups, (T) mean gene expression z-scores of immune checkpoint transcripts quantified in pooled day 21 B16F10 and day 24 KP tumors (n=6–23 per group, pooled from multiple independent experiments), (U) immune cell deconvolution analysis showing mean gene expression z-scores of activated dendritic cell specific transcripts (n=6–23 per group, pooled from multiple independent experiments). All error bars show SE, statistical tests used are t-test (A–C and E–O), Dunn's test (D, U) and one-way ANOVA (T). [+], stars indicate significance level of t-test compared with TRI-IT group, *p<0.05, **p<0.01, ***p<0.001, ****p<0.0001. ANOVA, analysis of variance; TRI-IT, tripartite immunotherapy. PBS, phosphate-buffered saline. KP: $Kras^{LSL\text{-}G12D}$ $p53^{fl/fl}$ lung cancer cell line. PLR, partial least square regression. FACS, fluorescence activated cell sorter. VIP: variable importance in projection.

as IL-3, IL-4, IL-17, IL-10, IL-6, IL-12(p70) and RANTES (figure 3P) in higher order combinations. Acknowledging the complex spatial and temporal context-dependency of cytokines,[54] the observed patterns could point to a possible rebalancing of host immunity towards Th2-polarization (IL-4, IL-6, IL-10),[55] myeloid-derived suppressor cell support (IL-17)[56] and M2-polarization of macrophages (IL4, IL-10)[57 58] on combination immunotherapy without

lymphodepletion. This signature was diminished with the full TRI-IT protocol including lymphodepletion while the likely beneficial, proinflammatory, Th1-polarizing signature elicited by TRI-IT subcomponents, was largely maintained.

To further understand the contribution of single cytokines to antitumor response with TRI-IT, we constructed a partial least squares regression model using peripheral cytokine concentrations as input predicting tumor size across treatment groups with high accuracy (figure 3Q). Cytokines associated with smaller tumors were IL-5, MIG, IFNγ, IL-2, MIP-1a, and MIP-1b. Cytokines associated with increased tumor growth were IL-4, IL-17, IL12p(70), RANTES and VEGF (figure 3R). Interestingly, this pattern of cytokines associated with larger tumors had significant overlap with those that were suppressed in the full TRI-IT protocol by the addition of lymphodepletion (figure 3P).

We used gene set enrichment analysis to investigate signatures of immune response, revealing significant enrichment of an adaptive, humoral, innate immune and inflammatory response signature in TRI-IT-treated mice (online supplemental figure S3).

Upregulation of alternative checkpoints has been recognized as an immunotherapy resistance mechanism.[59] Therefore, we compared intratumoral gene expression of CTLA4, HAVCR2, LAG3, TIGIT, and SIGLECG by 3'mRNAseq of bulk tumor tissue across groups. Interestingly, lower-order subcombinations of TRI-IT treatment elements led to varying upregulation of one or multiple of these alternative checkpoints, which was abrogated by TRI-IT (figure 3T). Presence of activated dendritic cells is crucial for a tumor-specific, adaptive immune response.[60] Quantified by immune cell deconvolution, tumors from mice treated with TRI-IT or the TLR+aPD1+ACT combination without lymphodepletion contained more activated dendritic cells than other groups (figure 3U).

Altogether, above experiments confirm that TRI-IT induces adaptive, humoral and cellular immune responses that are accompanied by a broadly increased infiltration of adaptive and innate effector cells into tumors and a systemic cytokine response characterized by an increase in inflammatory, Th1-response-associated cytokines and a decrease in immunosuppressive cytokines.

As soft tissue sarcomas are known to be refractory to immune checkpoint inhibitors, we sought to evaluate TRI-ITs efficacy in two separate models of murine KP-derived and chemically (MCA)-induced MCA/p53 sarcoma[61] (online supplemental figure S5A). We first confirmed tumor-specificity of CTLs (online supplemental figure S5B,C). In both sarcoma mouse models, we observed high efficacy of TRI-IT when treating established tumors (online supplemental figure S5D,E). Tumors from TRI-IT-treated mice exhibited higher infiltration of NK1.1+CD3+ cells, a trend towards higher infiltration of γδ-T and NK-cells and a lower infiltration of Tregs (online supplemental figure S5F). Tumors from TRI-IT-treated mice had a higher intra-tumoral CD8+/Treg-ratio (online supplemental figure S5G) and a trend towards an increase in intra-tumoral IFNγ+ cells among CD4+and CD8+T cells, γδ-T-cells, NK cells and NK1.1+CD3+cells (online supplemental figure S5H). Among circulating cytokines, IFNγ and MIG were significantly increased in TRI-IT-treated mice (online supplemental figure S5I) and associated with tumor response (online supplemental figure S5J). Overall, the observed immunological changes in the independent sarcoma models closely matched those in the KP lung and B16F10 models, pointing to universal and not model-specific changes induced by TRI-IT.

Additionally, we investigated the efficacy of TRI-IT in different allogeneic humanized mouse models of lymphoma, NSCLC and breast cancer demonstrating its efficacy in different lymphoma and oncogene-driven solid tumors (online supplemental figures S6A-G, S7A-D and S8A-C, online supplemental results).

Depletions of CD4+ and CD8+ T-cells, NK-cells, γδ-T-cells and macrophages reduce efficacy of TRI-IT

Next, we aimed to elucidate the contribution of immune cell subsets to the efficacy of TRI-IT by depleting them in TRI-IT-treated, B16F10-bearing mice (figure 4A). Depletions were confirmed by flow cytometry (online supplemental figure S9A). Surprisingly, depletions of either CD4+or CD8+T cells, NK-cells, γδ-T-cells or macrophages all decreased the therapeutic effect of TRI-IT (figure 4B).

To unravel the mechanism of the diminished efficacy of TRI-IT by the depletions, we quantified cellular and humoral antitumor immunity. Depletions of CD8+T cells, NK-cells and γδ-T-cells, all key mediators of adaptive or innate cellular immunity, led to reduced cellular antitumor immunity (figure 4C). Depletion of CD4+T cells, which are crucial for the induction of humoral immunity,[62] and γδ-T-cells led to the biggest reduction in humoral anti-tumor immunity (figure 4D).

Interestingly, in addition to absence of the depleted immune cell subtype, depletion of any immune cell subtype also led to a broadly reduced immune cell infiltration of tumors in general (figure 4E–I), suggesting that TRI-IT induced TIME changes depend on the presence of a broad spectrum of immune cells.

We further sought to confirm these findings in the humanized allogeneic H1975 lung cancer xenograft model. Reminiscent of the B16F10 model, depletion of CD4+ and CD8+cells resulted in decreased efficacy of TRI-IT (online supplemental figure S9B).

Taken together, we demonstrate that CD4+ and CD8+T cells, macrophages, NK-cells and γδ-T-cells are crucial for TRI-IT's efficacy.

TRI-IT displays high efficacy in autologous humanized patient-derived mouse models of lung cancer

Profound differences between murine and human immunity necessitate immunotherapy models that are as close as possible to human cancer. Preclinical evaluation of novel cancer treatments in models as close as possible to actual patients is vital. To this end, we evaluated TRI-IT's efficacy in autologous humanized cancer models.[63 64]

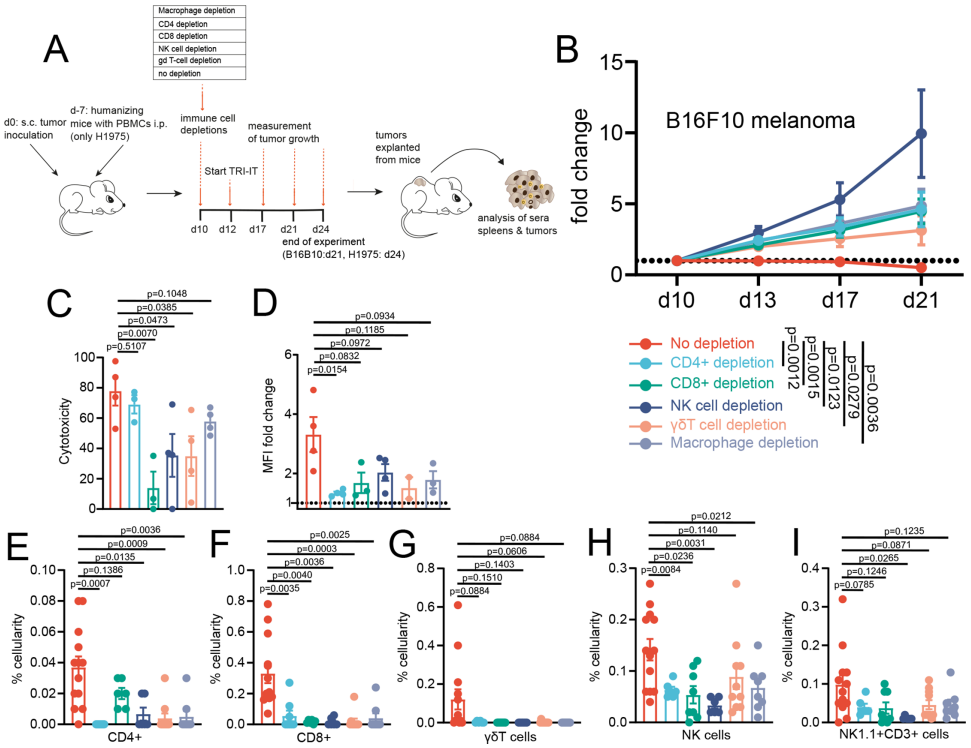

Figure 4 Depletions of CD4+ and CD8+ T cells, NK-cells, γδ-T-cells and macrophages reduce TRI-IT antitumor effect. (A) Experimental overview of in vivo experimental workflow, (B) mean fold change of subcutaneous B16F10 melanoma tumor volumes in C57BL/6J mice over time in indicated depletion groups (n=6–8 per group), (C) quantification of cellular anti-tumor immunity in splenocytes of B16F10 bearing C57BL/6J mice on day 21 in different treatment groups by measuring cytotoxicity towards B16F10 cells (n=3–4 per group, see the Methods section for details), (D) quantification of antitumor antibody response in sera of subcutaneous B16F10 bearing C57BL/6J mice on day 21 in different depletion groups shown as fold change of geometric mean fluorescence intensity measured by FACS compared with tumor-naïve control mice (n=2–4 per group, see the Methods section for details), (E–I) immune cell infiltration into subcutaneous B16F10 bearing C57BL/6J mice on day 21 in different depletion groups measured by FACS (n=8–13 per group, pooled from multiple independent experiments). all error bars show SE, statistical tests used are two tailed, unpaired t-tests (A, C–I) and two-way ANOVA (B). ANOVA, analysis of variance; TRI-IT, tripartite immunotherapy.

We created humanized PDX models from two different NSCLC patients (figure 5A) (online supplemental note).

We first confirmed specificity of autologous anti-PDX CTLs, revealing high specificity of especially CD8+CTLs towards their target PDX (figure 5B–D). Of note, CTLs generated from the same patient's PBMCs against early (PDX1.1) and late generation (PDX1.2) PDX were not cross-reactive. Consistent with our experiments in poorly immunogenic murine NSCLC we found a strong tumor response to TRI-IT compared with standard aPD1 monotherapy in all NSCLC PDX models (figure 5E–G).

As expected, TRI-IT-treated mice showed increased IFNγ and trends towards increased levels of TNFα, MIP-1a and MIP-1b in circulation (figure 5H). In line with our findings in murine B16F10 and KP models, we observed increased CD4+, CD8+ and γδ-T-cell infiltration into tumors in TRI-IT-treated mice (figure 5I) and a higher proportion of functionally active, IFNγ+ CD8+T-, NK- and CD56+CD3+cells (figure 5J). No significant difference between TLR-agonist-injected and non-TLR-agonist-injected tumors was observed (figure 5K), indicating possible abscopal effects of the local TLR agonist mix also in these models.

TRI-IT displays high efficacy in an autochthonous, genetically engineered lung cancer model

Finally, because the immune landscapes of transplanted tumors can differ from primary tumors that coevolve with the immune system,[65] we evaluated TRI-IT in the non-immunogenic, autochthonous, genetically defined KP model of lung cancer[40] (figure 6A). Intratumoral injection of the TLR agonist mix was not feasible intrapulmonary, therefore, we tested two adaptions of TRI-IT: injecting the TLR agonist mix subcutaneously and administering it via inhalation. We observed a very good tumor response to TRI-IT as assessed by micro-CT scan (μCT) compared with aPD1 treatment (figure 6B,C). TRI-IT-treated animals had less lung affected by tumor (figure 6D), less lesions per lung (figure 6E) and trended toward smaller tumors (figure 6F). Assessing infiltration of T-cells into autochthonous KP tumors by IHC (figure 6G), we found higher levels of T-cells in general and the CD4+T cell subset and a trend toward higher levels of CD8+T cells in TRI-IT-treated mice.

To evaluate changes in the TIME more comprehensively, we collected tumors at the end of the experiment and performed bulk tumor RNA-sequencing, followed

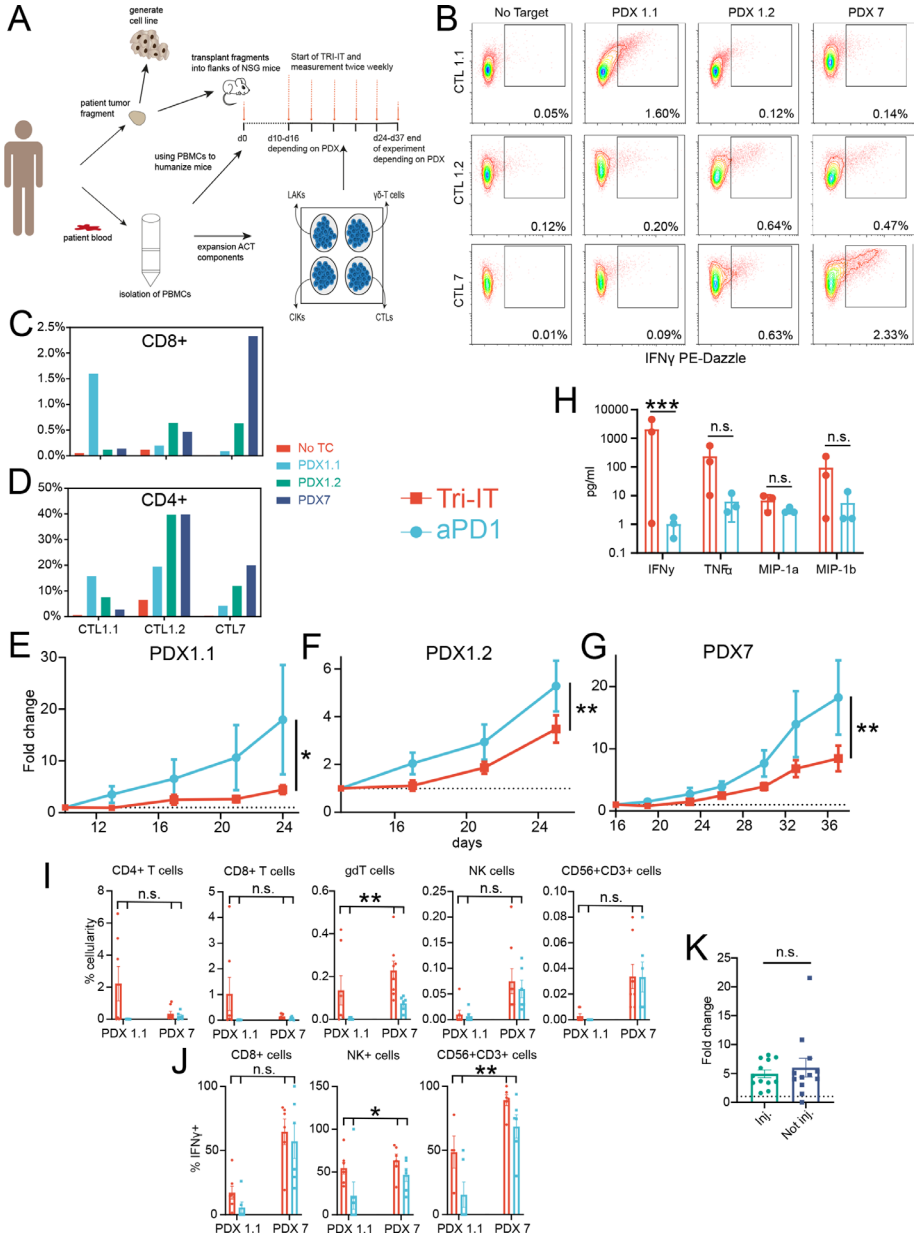

Figure 5 TRI-IT is effective in autologous humanized patient-derived mouse models of lung cancer. (A) Experimental overview of in vivo experimental workflow, (B) FACS plots showing proportion of intracellularly IFNγ+ cells among CD8+T cells after restimulation of indicated CTLs with either no target cells or indicated PDX cells, (C, D) Proportion of intracellularly IFNγ+ cells among CD8+ (C) or CD4+ (D) T-cells after restimulation of indicated CTLs with either no target cells or indicated PDX cells, (E–G) mean fold change of indicated PDX tumor growth in autologously humanized NSG mice over time in indicated treatment groups (n=5–8 per group), (H) mean levels of indicated cytokines quantified by multiplex Luminex analysis in the sera of PDX1.1 bearing autologously humanized NSG mice sacrificed on day 24 treated in indicated experimental groups (n=3 per group). (I) Immune cell infiltration on day 24 (PDX1) or day 37 (PDX7) into indicated PDX tumors growing in autologously humanized mice in indicated treatment groups measured by FACS (n=6–8 per group), (J) proportion of IFNγ+ cells among indicated subsets of tumor-infiltrating immune cells on day 24 (PDX1) or day 37 (PDX7) into indicated PDX tumors growing in autologously humanized mice in indicated treatment groups measured by intracellular FACS (n=6–7 per group), (K) comparison of injected versus not-injected tumor growth fold change at the end of the experiment in pooled PDX 1.1, PDX 1.2 or PDX 7 tumors (n=12 per group). All error bars show SE, statistical tests used are two tailed, unpaired t-test for (E–H) and two-way ANOVA with significance of the variable 'group allocation' reported (I–J). *p<0.05, **p<0.01, ***p<0.001. ANOVA, analysis of variance; PDX, patient-derived xenograft; TRI-IT, tripartite immunotherapy.

by immune cell deconvolution. Intratumoral inactivated and activated dendritic cells, macrophages, neutrophils, B-cells, Th1, Th2 and Tfh cells and CD56dim NK cells were increased in TRI-IT with inhaled TLR agonist mix-treated compared with aPD1-treated mice (figure 6H). Examination of intratumoral cytokine and chemokine transcripts revealed an increased Th1-response associated, inflammatory and chemoattractant-rich signature in TRI-IT

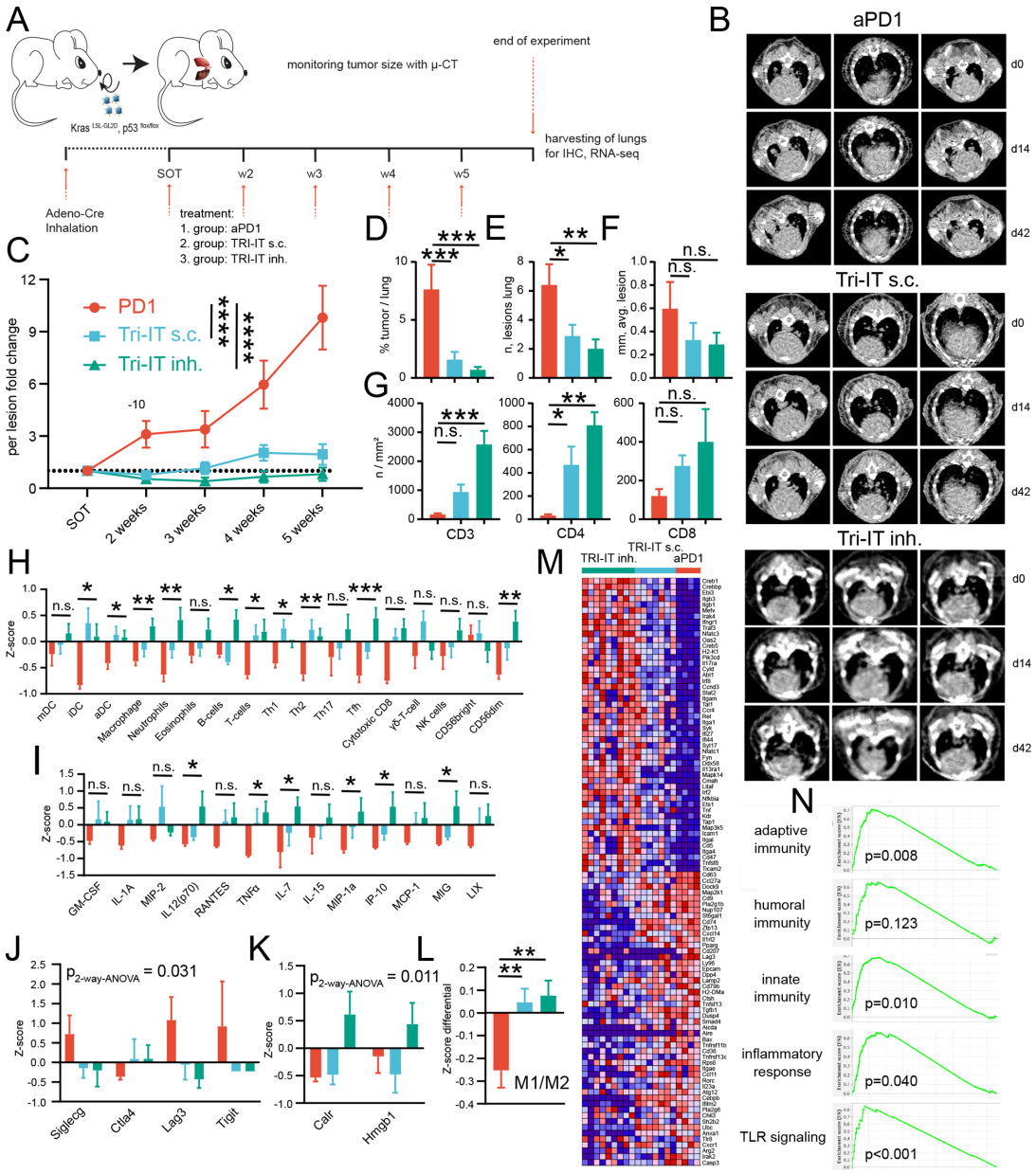

Figure 6 TRI-IT shows synergistic treatment effects in an autochthonous genetically engineered lung cancer mouse model. (A) Experimental overview of in vivo experimental workflow, (B) representative µCT images of autochthonous KP lung cancers in indicated treatment groups at indicated times after treatment initiation, (C) mean fold change of autochthonous KP lung cancer lesion growth over time in indicated treatment groups (n=8–29 lesions per group), (D–F) indicated measures of tumor burden at end of experiment measured on H&E-stained coronal cuts through both lungs (n=5–8 mice per group), (G) infiltration of tumors by indicated immune cell subsets at end of experiment measured on IHC of coronal cuts through both lungs (n=4–7 mice per group), (H) immune cell deconvolution analysis showing mean gene expression z-scores of immune cell specific transcripts (n=4–9 mice per group, see the Methods section for details), (I) mean gene expression z-scores of intratumoral cytokines and chemokines (n=4–9 mice per group), (J) mean gene expression z-scores of selected immune checkpoint transcripts (n=4–9 mice per group), (K) mean gene expression z-scores of transcripts representative of a immunogenic cell death signature (n=4–9 mice per group), (L) mean differential gene expression z-score of transcripts representative of a M1/M2 macrophage signature indication M2 to M1 shift (n=4–9 mice per group, see the Methods section for details), (M) heatmap showing most differentially expressed transcripts (aPD1 vs any TRI-IT) (n=4–9 mice per group), (N) gene set enrichment analysis for selected gene sets from any TRI-IT versus aPD1 treated autochthonous KP lung tumors. All error bars show SEM, statistical tests used are a mixed-effects model (C), t-tests between indicated groups (D–I, L) and two-way ANOVA with significance of the variable 'group allocation' reported (J–K) . *p<0.05, **p<0.01, ***p<0.001, ****p<0.0001. ANOVA, analysis of variance; IHC, immunohistochemistry; ns, not significant; TRI-IT, tripartite immunotherapy.

with inhaled TLR agonist mix-treated compared with aPD1-treated mice (figure 6I). As in previous models (figure 3T), alternative immune checkpoints were not upregulated, but rather downregulated by TRI-IT in autochthonous KP lung cancer (figure 6J).

Induction of immunogenic cell death has been described as a key goal of combination immunotherapy.[66] Interestingly, increased transcripts representative of an immunogenic cell death signature, point towards induction of immunogenic cell death by TRI-IT (figure 6K). Analysis of differential M1 and M2 polarization signatures by 3'mRNAseq revealed a shift towards M1 polarization on TRI-IT treatment (figure 6L).

Examining differentially expressed transcripts between TRI-IT- and aPD1-treated mice, we observed increased transcripts of dsRNA targets (OAS2), chemokine receptors (CCR4), and genes involved in T-cell and neutrophil activation (PIK3CD), innate immune responses to TLR activation (IRAK4) and antigen presentation (TAP1). Interestingly, we also observed a reduced transcript frequency of negative regulators of anti-tumor immune responses in TRI-IT-treated mice, such as ARG2 or LAG3 and of genes involved in induction of antigen tolerance (AIRE) (figure 6N). Finally, we used gene set enrichment analysis to investigate signatures of immune response. This analysis revealed a strong enrichment of gene sets representing an adaptive, humoral, innate and inflammatory response as well as increased TLR signaling (figure 6O).

Inhaled delivery of the TLR agonist mix led to better tumor control than subcutaneous delivery (figure 6B–F). This was matched by higher levels of broad intratumoral immune cell infiltration (figure 6G,H), an even more beneficial intratumoral cytokine and chemokine profile (figure 6I) and a further increased immunogenic cell death signature (figure 6K). We conclude that inhaled delivery of TLR agonists as part of TRI-IT is a highly feasible and effective option for the treatment of lung tumors.

In summary, our findings in autologous PDX models and the poorly immunogenic, autochthonous KP lung cancer model confirmed the efficacy of TRI-IT, with local and systemic changes induced by TRI-IT that were largely similar to those observed in the B16F10 melanoma and KP lung cancer models.

TRI-IT is not associated with off-target toxicity

Combination immunotherapy has been associated with profound toxicity.[67] Therefore, we aimed to evaluate common toxicities associated with combination immunotherapy in mice. We compared weight loss, organ weight and CD3+T cell infiltration into organs as surrogates for off-target immune-mediated toxicity between TRI-IT and control treated animals with or without subcutaneous B16F10 melanomas (figure 7A). Reassuringly, we found only a minimal, non-significant (≈ 3%) difference in weight change between TRI-IT and IgG/PBS (phosphate-buffered saline) treated animals (figure 7B) and no difference in lung weight (figure 7C), liver weight (figure 7D), spleen weight (figure 7E) and CD3+T cell infiltration into liver (figure 7F,G), lung (figure 7H,I) and colon (figure 7J,K). Altogether, these results indicate that TRI-IT is safe and has low off-target immune-mediated toxicity.

DISCUSSION

We here develop an antigen-agnostic, tripartite combination immunotherapy named TRI-IT that is effective in a wide range of poorly immunogenic tumors for which a precise antigenic determinant is not known. Until now, most combination immunotherapy approaches that are effective in poorly immunogenic tumors rely on precise knowledge of the antigenic determinants of a tumor and include adoptively transferred cells, vaccinations or antibodies engineered to directly target those.[8 21]

TRI-IT consists of three elements, combining checkpoint blockade targeting PD1, local immunotherapy by injection of agonists against TLR 3, 7 and 9 into one tumor lesion and an optimized combined ACT protocol including LAKs, CIKs, γδ-T-cells and tumor-specific CTLs following lymphodepletion.

In a first step, we show that our combined ACT protocol was superior to ACT with only LAKs, CIKs, γδ-T-cells or tumor-specific CTLs. Most of the elements of our combined ACT protocol have been tested in clinical trials as single elements, often with mixed results.[24 28 68] Surprisingly, combination treatments of these effector cells have not been studied so far in depth, despite, in our view, a good rationale for it. Our data show that combination ACT of adaptive and innate immune cells contributes to a higher infiltration of macrophages, T-cells, Th1, Th2 and Th17 polarized T-cells, Tfh-cells, cytotoxic T-cells and γδ-T-cells into the tumor. Moreover it induced a broad increase in important antitumor chemokines and cytokines both in the TIME and systemically, indicating that combined ACT induces a Th1-polarized immune response, increased NK and T-cell activity, proliferation and survival.[45 46] In contrast, we hypothesize that single cell type ACT efficacy might be limited due to high levels of systemic immunosuppressive cytokines (eg, IL10)[47] or LIX, which has recently been described as tumor growth and metastasis promoting.[48 49]

After having optimized the combined ACT protocol, we expanded it to the full TRI-IT protocol including systemic PD1 checkpoint blockade, local TLR stimulation and pre-ACT lymphodepletion. We show in syngeneic mouse models that TRI-IT can cure established, poorly immunogenic tumors and induces durable antitumor immunity by inducing broad adaptive humoral and cellular immune responses. Thus, functionally, adaptive cellular and humoral, as well as innate anti-tumor immune responses are coactivated to mediate the antitumor effect of TRI-IT. While tumor-specific T-cells are transferred to the host as part of TRI-IT and likely expand in the host, no tumor-specific antibodies are transferred, indicating that TRI-IT induces endogenous anti-tumor antibody responses, which have been recognized as an important

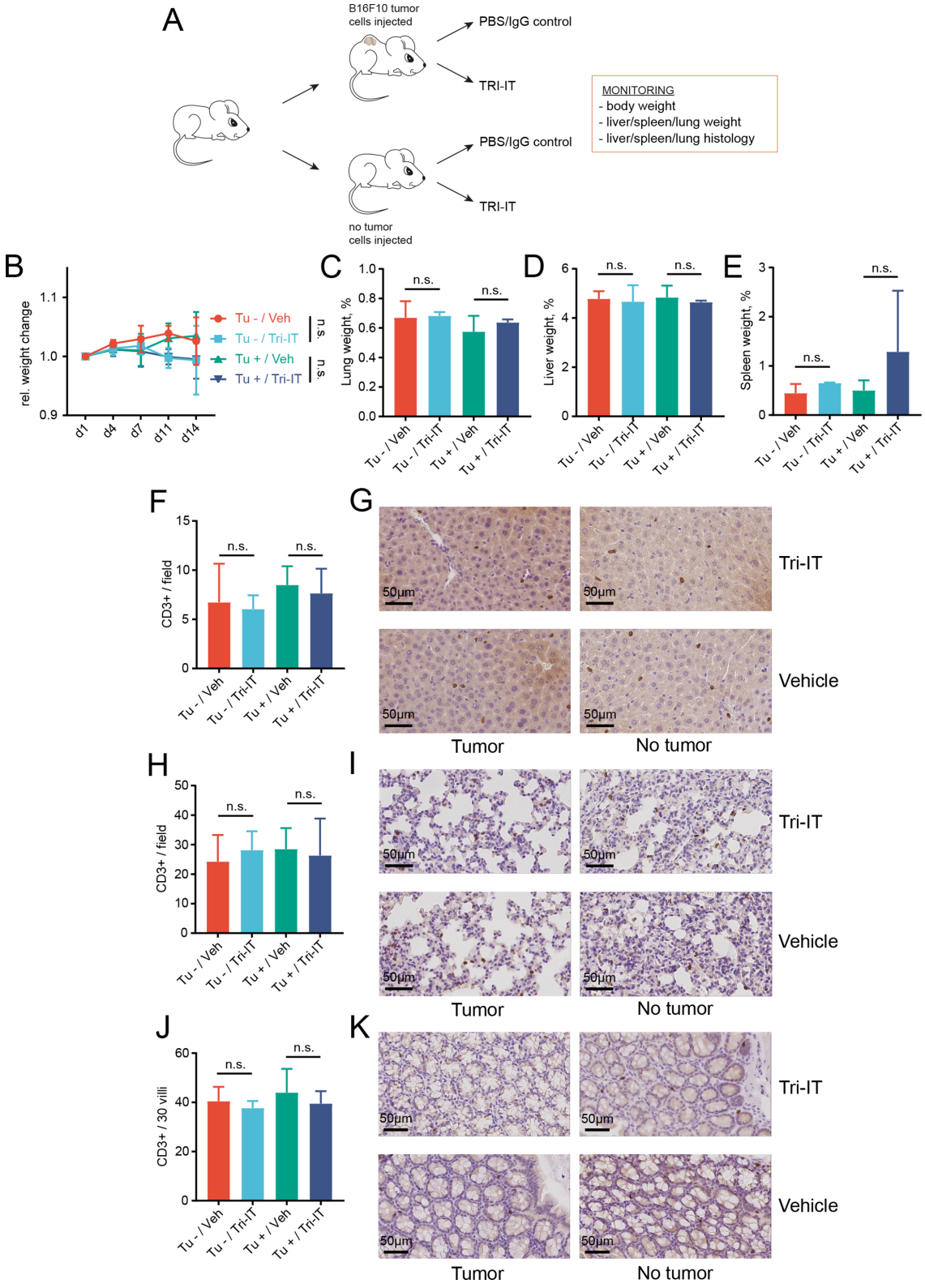

Figure 7 TRI-IT exhibits no off-target, immune-mediated toxicity. (A) Experimental overview of in vivo experimental workflow, (B) mean relative weight change of mice in indicated groups over time (n=4 per group), (C–E) lung (C), liver (D) or spleen (E) weight in percent of body weight at the end of experiment (day 14) in indicated groups (n=4 per group), Tu: tumor, (F, G) enumeration (F) of CD3+T cells infiltrating the liver per field of view by immunohistochemistry and accompanying representative (G) images (n=3–4 per group), (H, I) enumeration (H) of CD3+T cells infiltrating the lung per field of view by immunohistochemistry and accompanying representative (I) images (n=3–4 per group), (J, K) enumeration (J) of CD3+T cells infiltrating the intestine per 30 villi by immunohistochemistry and accompanying representative (K) images (n=3–4 per group). All error bars show SEM, statistical tests used are two-sided, unpaired t-tests (B–E, F, H and J). ns, not significant; TRI-IT, tripartite immunotherapy.

element of antitumor immune activity.[69 70] Our depletion studies show that TRI-IT relies on both innate and adaptive immunity. This is in line with recent studies that have shown improved immunotherapy efficacy if innate and adaptive immune responses are simultaneously harnessed.[71 72]

To evaluate TRI-IT in preclinical models as close to the patient as possible, we evaluated TRI-IT in autologous PDX models from lung cancer patients and confirmed its efficacy. Autochthonous cancer models usually respond poorly to immunotherapy.[50] Therefore, we also evaluated, as a final test, TRI-IT in the poorly immunogenic, autochthonous KP lung cancer model, again demonstrating its efficacy and mode of action.

All three elements of TRI-IT contributed variously to its efficacy in different models, with the full combination required to eradicate established tumors. Lymphodepletion prior to ACT seems to be crucial for the efficacy of TRI-IT, which is in line with existing evidence that lymphodepleting host preparation is crucial for ACT efficacy.[34]

Notably, we show that an inhaled variant of local immune stimulation with TLRs in our autochthonous NSCLC model is a highly effective method to deliver TLRs intrapulmonary to tumor lesions. Despite being complex, our approach can be easily translated into clinical trials, as all elements have already been tested in humans. Compared with established oncological treatment approaches such as allogeneic stem cell transplantation for hematological cancers, TRI-IT has manageable complexity. Each component of our combined ACT protocol has been evaluated in clinical trials and deemed safe,[24 68 73] apart from the CTL component, however, we do not expect increased toxicity compared with treatment with conceptually similar TILs, which have also been evaluated in many trials in different clinical settings.[74] The same holds true for locally applied TLR agonists[14 75 76] and systemic aPD1 treatment.[4] Furthermore, we evaluated toxicity of the full TRI-IT in mice and observed no off-target immunotoxicity.

In summary, our data indicate that TRI-IT is a clinically translatable, universal combination immunotherapy that is antigen-agnostic and highly efficient in a variety of poorly immunogenic tumor models inducing broad adaptive, innate and humoral anti-tumor responses and lasting anti-tumor immunity without prior knowledge of an antigenic determinant.

Author affiliations
[1]Department I of Internal Medicine, Center for Integrated Oncology Aachen Bonn Cologne Duesseldorf, University of Cologne, Cologne, Germany
[2]Center for Molecular Medicine, University of Cologne, Cologne, Germany
[3]Department of Cardiothoracic Surgery, University of Cologne, Cologne, Germany
[4]Mildred Scheel School of Oncology, University Hospital Cologne, Medical Faculty, Cologne, Germany
[5]Institute of Pathology, University of Cologne, Cologne, Germany
[6]Department of Radiation Oncology and Department of Pharmacology and Cancer Biology, Duke University Medical Center, Durham, North Carolina, USA
[7]Institute of Transfusion Medicine, University of Cologne, Cologne, Germany
[8]Department of General, Visceral and Cancer Surgery, University of Cologne, Cologne, Germany
[9]Department of Hematology and Stem Cell Transplantation, University Hospital Essen,University Duisburg-Essen, German Cancer Consortium (DKTK partner site Essen), Essen, Germany

Twitter H. Christian Reinhardt @chr_reinhardt

Acknowledgements We are indebted to our patients, who provided primary material.

Contributors Conceptualization, SB; methodology, SB, PL, JF, RTU investigation, all authors. Formal analysis, SB, writing–original draft, SB and RTU; writing, review and editing: all authors. Funding acquisition, SB, JB, AJW, DK, CR, and RTU; Guarantor and supervision: SB and RTU.

Funding This work was funded through the German-Israeli Foundation for Research and Development (I-65-412.20-2016 to CR), the Deutsche Forschungsgemeinschaft (EN 179/13-1 to SB, KFO-286-RP2, RE 2246/13-1, SFB-1399-A01/C02 to CR), the Else Kröner-Fresenius Stiftung (EKFS-2014-A06 to CR, 2016_Kolleg.19 to CR, SB, Memorial Grant 2018_EKMS.35 to JB), the Frauke Weiskam + Christel Ruranski-Stiftung (T0136-33.661 to SB), the Deutsche Krebshilfe (1117240 and 70113041 to CR, 70113307 to JB, 70113009 to RTU), the Thyssen Foundation (10.16.1.028 MN to RTU), the Nachwuchsforschungsgruppen NRW grant (1411ng005 to RTU) and the German Ministry of Education and Research (BMBF e:Med 01ZX1303A to CR). DK was supported by R35 CA197615 and AJW was supported by F30 CA221268.

Competing interests SB has received travel support from BMS and travel support and consulting fees from Takeda. SB received research funding form Takeda, but this funding did not support the research described in this paper. DK is a cofounder of XRAD Therapeutics, which is developing radiosensitizers. DK is the recipient of a Stand Up To Cancer (SU2C) Merck Catalyst Grant studying pembrolizumab and radiation therapy in sarcoma patients. DK has received research funding from XRAD Therapeutics, Eli Lilly & Co., Bristol Myers Squibb, Varian Medical Systems, and Merck, but this funding did not support the research described in this paper. CR received consulting and lecture fees from Abbvie, Astra-Zeneca, Vertex and Merck. CR received research funding from Gilead Pharmaceuticals. CR is a cofounder of CDL Therapeutics.

Patient consent for publication Not applicable.

Ethics approval All human subject research (PDX generation, PBMC donation) was performed in accordance with approved protocols by the local ethics committee (Cologne University Hospital) and the Declaration of Helsinki.

Provenance and peer review Not commissioned; externally peer reviewed.

Data availability statement Data are available in a public, open access repository. Data are available on reasonable request. The data that support the findings of this study are available from the corresponding author on reasonable request. RNA-sequencing data have been uploaded to GEO under the accession number GSE173107.

ORCID iD
Sven Borchmann http://orcid.org/0000-0001-6662-6864

REFERENCES

1 Ferlay J, Colombet M, Soerjomataram I, *et al*. Estimating the global cancer incidence and mortality in 2018: GLOBOCAN sources and methods. *Int J Cancer* 2019;144:1941–53.

2 Mellman I, Coukos G, Dranoff G. Cancer immunotherapy comes of age. *Nature* 2011;480:480–9.
3 Waldman AD, Fritz JM, Lenardo MJ. A guide to cancer immunotherapy: from T cell basic science to clinical practice. *Nat Rev Immunol* 2020;20:651–68.
4 Topalian SL, Hodi FS, Brahmer JR, *et al*. Safety, activity, and immune correlates of anti-PD-1 antibody in cancer. *N Engl J Med* 2012;366:2443–54.
5 Moynihan KD, Irvine DJ. Roles for innate immunity in combination immunotherapies. *Cancer Res* 2017;77:5215–21.
6 Carbone DP, Reck M, Paz-Ares L, *et al*. First-Line nivolumab in stage IV or recurrent non-small-cell lung cancer. *N Engl J Med* 2017;376:2415–26.
7 Binnewies M, Roberts EW, Kersten K, *et al*. Understanding the tumor immune microenvironment (time) for effective therapy. *Nat Med* 2018;24:541–50.
8 Moynihan KD, Opel CF, Szeto GL, *et al*. Eradication of large established tumors in mice by combination immunotherapy that engages innate and adaptive immune responses. *Nat Med* 2016;22:1402–10.
9 Ansell SM, Lesokhin AM, Borrello I, *et al*. Pd-1 blockade with nivolumab in relapsed or refractory Hodgkin's lymphoma. *N Engl J Med* 2015;372:311–9.
10 Gandhi L, Rodríguez-Abreu D, Gadgeel S, *et al*. Pembrolizumab plus chemotherapy in metastatic non-small-cell lung cancer. *N Engl J Med* 2018;378:2078–92.
11 Kaczanowska S, Joseph AM, Davila E. Tlr agonists: our best frenemy in cancer immunotherapy. *J Leukoc Biol* 2013;93:847–63.
12 Shojaei H, Oberg H-H, Juricke M, *et al*. Toll-Like receptors 3 and 7 agonists enhance tumor cell lysis by human gammadelta T cells. *Cancer Res* 2009;69:8710–7.
13 Salazar AM, Erlich RB, Mark A, *et al*. Therapeutic in situ autovaccination against solid cancers with intratumoral poly-ICLC: case report, hypothesis, and clinical trial. *Cancer Immunol Res* 2014;2:720–4.
14 Frega G, Wu Q, Le Naour J, *et al*. Trial Watch: experimental TLR7/TLR8 agonists for oncological indications. *Oncoimmunology* 2020;9:1796002.
15 Vollmer J, Weeratna R, Payette P, *et al*. Characterization of three CpG oligodeoxynucleotide classes with distinct immunostimulatory activities. *Eur J Immunol* 2004;34:251–62.
16 Frank MJ, Reagan PM, Bartlett NL, *et al*. *In Situ* Vaccination with a TLR9 Agonist and Local Low-Dose Radiation Induces Systemic Responses in Untreated Indolent Lymphoma. *Cancer Discov* 2018;8:1258–69.
17 Gallotta M, Assi H, Degagné Émilie, *et al*. Inhaled TLR9 Agonist Renders Lung Tumors Permissive to PD-1 Blockade by Promoting Optimal $CD4^+$ and $CD8^+$ T-cell Interplay. *Cancer Res* 2018;78:4943–56.
18 Wesch D, Beetz S, Oberg H-H, *et al*. Direct costimulatory effect of TLR3 ligand poly(I:C) on human gamma delta T lymphocytes. *J Immunol* 2006;176:1348–54.
19 Krieg AM. Toll-Like receptor 9 (TLR9) agonists in the treatment of cancer. *Oncogene* 2008;27:161–7.
20 Zhao BG, Vasilakos JP, Tross D, *et al*. Combination therapy targeting toll like receptors 7, 8 and 9 eliminates large established tumors. *J Immunother Cancer* 2014;2:12.
21 Amos SM, Pegram HJ, Westwood JA, *et al*. Adoptive immunotherapy combined with intratumoral TLR agonist delivery eradicates established melanoma in mice. *Cancer Immunol Immunother* 2011;60:671–83.
22 Sivick KE, Desbien AL, Glickman LH, *et al*. Magnitude of Therapeutic STING Activation Determines $CD8^+$ T Cell-Mediated Anti-tumor Immunity. *Cell Rep* 2018;25:3074–85.
23 Rosenberg SA, Lotze MT, Muul LM, *et al*. A progress report on the treatment of 157 patients with advanced cancer using lymphokine-activated killer cells and interleukin-2 or high-dose interleukin-2 alone. *N Engl J Med* 1987;316:889–97.
24 Law TM, Motzer RJ, Mazumdar M, *et al*. Phase III randomized trial of interleukin-2 with or without lymphokine-activated killer cells in the treatment of patients with advanced renal cell carcinoma. *Cancer* 1995;76:824–32.
25 Schmidt-Wolf IG, Negrin RS, Kiem HP, *et al*. Use of a scid mouse/human lymphoma model to evaluate cytokine-induced killer cells with potent antitumor cell activity. *J Exp Med* 1991;174:139–49.
26 Schmidt-Wolf IG, Lefterova P, Mehta BA, *et al*. Phenotypic characterization and identification of effector cells involved in tumor cell recognition of cytokine-induced killer cells. *Exp Hematol* 1993;21:1673–9.
27 Leemhuis T, Wells S, Scheffold C, *et al*. A phase I trial of autologous cytokine-induced killer cells for the treatment of relapsed Hodgkin disease and non-Hodgkin lymphoma. *Biol Blood Marrow Transplant* 2005;11:181–7.
28 Takayama T, Sekine T, Makuuchi M, *et al*. Adoptive immunotherapy to lower postsurgical recurrence rates of hepatocellular carcinoma: a randomised trial. *Lancet* 2000;356:802–7.
29 Ribot JC, Lopes N, Silva-Santos B. γδ T cells in tissue physiology and surveillance. *Nat Rev Immunol* 2021;21:221–32.
30 Xu Y, Xiang Z, Alnaggar M, *et al*. Allogeneic Vγ9Vδ2 T-cell immunotherapy exhibits promising clinical safety and prolongs the survival of patients with late-stage lung or liver cancer. *Cell Mol Immunol* 2021;18:427–39.
31 Kabelitz D, Serrano R, Kouakanou L, *et al*. Cancer immunotherapy with γδ T cells: many paths ahead of US. *Cell Mol Immunol* 2020;17:925–39.
32 Cattaneo CM, Dijkstra KK, Fanchi LF, *et al*. Tumor organoid–T-cell coculture systems. *Nat Protoc* 2020;15:15–39.
33 Dijkstra KK, Cattaneo CM, Weeber F, *et al*. Generation of Tumor-Reactive T cells by co-culture of peripheral blood lymphocytes and tumor organoids. *Cell* 2018;174:1586–98.
34 Dudley ME, Wunderlich JR, Yang JC, *et al*. Adoptive cell transfer therapy following non-myeloablative but Lymphodepleting chemotherapy for the treatment of patients with refractory metastatic melanoma. *JCO* 2005;23:2346–57.
35 Schuster SJ, Bishop MR, Tam CS, *et al*. Tisagenlecleucel in adult relapsed or refractory diffuse large B-cell lymphoma. *N Engl J Med* 2019;380:45–56.
36 The R foundation for statistical computing R version 3.3.2.. Available: https://www.r-project.org/
37 GraphPad software. *GraphPad prism*. La Jolla, CA, 2022.
38 Golfmann K, Meder L, Koker M, *et al*. Synergistic anti-angiogenic treatment effects by dual FGFR1 and VEGFR1 inhibition in FGFR1-amplified breast cancer. *Oncogene* 2018;37:5682.
39 Shaw R, Miller S, Curwen J, *et al*. Design, analysis and reporting of tumor models. *Lab Anim* 2017;46:207–11.
40 DuPage M, Dooley AL, Jacks T. Conditional mouse lung cancer models using adenoviral or lentiviral delivery of Cre recombinase. *Nat Protoc* 2009;4:1064–72.
41 Newman AM, Liu CL, Green MR, *et al*. Robust enumeration of cell subsets from tissue expression profiles. *Nat Methods* 2015;12:453–7.
42 Mulé JJ, Shu S, Schwarz SL, *et al*. Adoptive immunotherapy of established pulmonary metastases with LAK cells and recombinant interleukin-2. *Science* 1984;225:1487–9.
43 Kondo M, Sakuta K, Noguchi A, *et al*. Zoledronate facilitates large-scale ex vivo expansion of functional γδ T cells from cancer patients for use in adoptive immunotherapy*. *Cytotherapy* 2008;10:842–56.
44 Sanmamed MF, Chester C, Melero I, *et al*. Defining the optimal murine models to investigate immune checkpoint blockers and their combination with other immunotherapies. *Ann Oncol* 2016;27:1190–8.
45 Mazzucchelli R, Durum SK. Interleukin-7 receptor expression: intelligent design. *Nat Rev Immunol* 2007;7:144–54.
46 Santana Carrero RM, Beceren-Braun F, Rivas SC, *et al*. Il-15 is a component of the inflammatory milieu in the tumor microenvironment promoting antitumor responses. *Proc Natl Acad Sci U S A* 2019;116:599–608.
47 Dennis KL, Blatner NR, Gounari F, *et al*. Current status of interleukin-10 and regulatory T-cells in cancer. *Curr Opin Oncol* 2013;25:637–45.
48 Zhao J, Ou B, Han D, *et al*. Tumor-Derived CXCL5 promotes human colorectal cancer metastasis through activation of the ERK/Elk-1/Snail and AKT/GSK3β/β-catenin pathways. *Mol Cancer* 2017;16:70.
49 Romero-Moreno R, Curtis KJ, Coughlin TR, *et al*. The CXCL5/CXCR2 axis is sufficient to promote breast cancer colonization during bone metastasis. *Nat Commun* 2019;10:1–14.
50 Pfirschke C, Engblom C, Rickelt S, *et al*. Immunogenic chemotherapy sensitizes tumors to checkpoint blockade therapy. *Immunity* 2016;44:343–54.
51 Reilley MJ, Morrow B, Ager CR, *et al*. Tlr9 activation cooperates with T cell checkpoint blockade to REGRESS poorly immunogenic melanoma. *J Immunother Cancer* 2019;7:323.
52 Magen A, Nie J, Ciucci T, *et al*. Single-Cell Profiling Defines Transcriptomic Signatures Specific to Tumor-Reactive versus Virus-Responsive $CD4^+$ T Cells. *Cell Rep* 2019;29:3019–32.
53 Curran MA, Montalvo W, Yagita H, *et al*. PD-1 and CTLA-4 combination blockade expands infiltrating T cells and reduces regulatory T and myeloid cells within B16 melanoma tumors. *Proc Natl Acad Sci U S A* 2010;107:4275–80.
54 Cytokines in the balance. *Nat Immunol* 2019;20:1557.
55 Kaiko GE, Horvat JC, Beagley KW, *et al*. Immunological decision-making: how does the immune system decide to mount a helper T-cell response? *Immunology* 2008;123:326–38.

56 He D, Li H, Yusuf N, *et al*. Il-17 promotes tumor development through the induction of tumor promoting microenvironments at tumor sites and myeloid-derived suppressor cells. *J Immunol* 2010;184:2281–8.
57 Biswas SK, Mantovani A. Macrophage plasticity and interaction with lymphocyte subsets: cancer as a paradigm. *Nat Immunol* 2010;11:889–96.
58 Ohtaki Y, Ishii G, Nagai K, *et al*. Stromal macrophage expressing CD204 is associated with tumor aggressiveness in lung adenocarcinoma. *J Thorac Oncol* 2010;5:1507–15.
59 Jenkins RW, Barbie DA, Flaherty KT. Mechanisms of resistance to immune checkpoint inhibitors. *Br J Cancer* 2018;118:9–16.
60 Wculek SK, Cueto FJ, Mujal AM, *et al*. Dendritic cells in cancer immunology and immunotherapy. *Nat Rev Immunol* 2020;20:7–24.
61 Lee C-L, Mowery YM, Daniel AR, *et al*. Mutational landscape in genetically engineered, carcinogen-induced, and radiation-induced mouse sarcoma. *JCI Insight* 2019;4:e128698.
62 Elong Ngono A, Young MP, Bunz M, *et al*. Cd4+ T cells promote humoral immunity and viral control during Zika virus infection. *PLoS Pathog* 2019;15:e1007474.
63 Jespersen H, Lindberg MF, Donia M, *et al*. Clinical responses to adoptive T-cell transfer can be modeled in an autologous immune-humanized mouse model. *Nat Commun* 2017;8:707.
64 Choi Y, Lee S, Kim K, *et al*. Studying cancer immunotherapy using patient-derived xenografts (PDXs) in humanized mice. *Exp Mol Med* 2018;50:1–9.
65 Wisdom AJ, Mowery YM, Hong CS, *et al*. Single cell analysis reveals distinct immune landscapes in transplant and primary sarcomas that determine response or resistance to immunotherapy. *Nat Commun* 2020;11:6410.
66 Smyth MJ, Ngiow SF, Ribas A, *et al*. Combination cancer immunotherapies tailored to the tumour microenvironment. *Nat Rev Clin Oncol* 2016;13:143–58.
67 Larkin J, Chiarion-Sileni V, Gonzalez R, *et al*. Combined nivolumab and ipilimumab or monotherapy in untreated melanoma. *N Engl J Med* 2015;373:23–34.
68 Kakimi K, Matsushita H, Masuzawa K, *et al*. Adoptive transfer of zoledronate-expanded autologous Vγ9Vδ2 T-cells in patients with treatment-refractory non-small-cell lung cancer: a multicenter, open-label, single-arm, phase 2 study. *J Immunother Cancer* 2020;8:e001185.
69 Montgomery RB, Makary E, Schiffman K, *et al*. Endogenous anti-HER2 antibodies block HER2 phosphorylation and signaling through extracellular signal-regulated kinase. *Cancer Res* 2005;65:650–6.
70 Dieu-Nosjean M-C, Giraldo NA, Kaplon H, *et al*. Tertiary lymphoid structures, drivers of the anti-tumor responses in human cancers. *Immunol Rev* 2016;271:260–75.
71 Zhu EF, Gai SA, Opel CF, *et al*. Synergistic innate and adaptive immune response to combination immunotherapy with anti-tumor antigen antibodies and extended serum half-life IL-2. *Cancer Cell* 2015;27:489–501.
72 Yang X, Zhang X, Fu ML, *et al*. Targeting the tumor microenvironment with interferon-β bridges innate and adaptive immune responses. *Cancer Cell* 2014;25:37–48.
73 Laport GG, Sheehan K, Baker J, *et al*. Adoptive immunotherapy with cytokine-induced killer cells for patients with relapsed hematologic malignancies after allogeneic hematopoietic cell transplantation. *Biol Blood Marrow Transplant* 2011;17:1679–87.
74 Dafni U, Michielin O, Lluesma SM, *et al*. Efficacy of adoptive therapy with tumor-infiltrating lymphocytes and recombinant interleukin-2 in advanced cutaneous melanoma: a systematic review and meta-analysis. *Ann Oncol* 2019;30:1902–13.
75 Le Naour J, Galluzzi L, Zitvogel L, *et al*. Trial Watch: TLR3 agonists in cancer therapy. *Oncoimmunology* 2020;9:1771143.
76 Smith M, García-Martínez E, Pitter MR, *et al*. Trial Watch: Toll-like receptor agonists in cancer immunotherapy. *Oncoimmunology* 2018;7:e1526250.